RSC Advances

PAPER

View Article Online
View Journal | View Issue

Cite this: *RSC Adv.*, 2020, **10**, 332

Multi-ionization of the Cl_2 molecule in the near-infrared femtosecond laser field

Jian Zhang,[a] Zhipeng Li[b] and Yan Yang *[b]

Received 27th August 2019
Accepted 2nd December 2019

DOI: 10.1039/c9ra06746a

rsc.li/rsc-advances

The multi-electron ionization and subsequent dissociation of the Cl_2 molecule in a near-infrared femtosecond laser field was investigated *via* the dc-sliced ion imaging technique. The single charged molecular ions, Cl_2^+, dissociate from two excited states, $^2\Pi_u$ and $^2\Sigma_g^+$, with the electrons ionized from the HOMO−1 and HOMO−2 orbital, respectively. For the multi-charged molecular ions, Cl_2^{n+} (n = 2–8), our results showed that the stretch of the inter-nuclear distance benefitted the ionization of the electrons to produce highly-charged molecular ions. In addition, compared with the traditional charge resonance enhanced ionization (CREI) model, the critical distance (R_c) for the Cl_2 molecule in our experiment was a short range that depended on the charge state rather than a single point.

Introduction

Diatomic molecules, which are exposed to a femtosecond laser field with an intensity over 10^{14} W cm^{-2}, always undergo multi-electron dissociative ionization, followed by the explosion of molecular ions into ionic fragments with characteristic kinetic energy releases (KERs).[1–8]

Recently, multi-electron ionization in an intense field has drawn extensive attention. At the same time, some theoretical models have been proposed to illustrate the dynamical process. The multi-electron dissociative ionization (MEDI) model showed that the femtosecond laser field can quickly strip several electrons off at the equilibrium nuclear distance. The subsequent dissociation of the charged molecular ion was influenced by the repulsive Coulomb energy. However, the energy defect, namely, the kinetic energy releases (KERs) was always smaller than the theoretical prediction for all of the charged states of the molecular ions, is still indistinct and unresolved. For last two decades, several models have been proposed to explain this issue. The post-dissociative ionization (PDI) model showed that the fragment ions could be ionized for the second time after the dissociation process.[9] This model explained the origin of high charged fragmental ions with small kinetic energy. S. Chelkowski and A. D. Bandrauk proposed a two-step model in which the molecule loses electrons and coulomb explosions occur twice, at their equilibrium distance and critical distance.[10] This model explains the energy defect problem from the starting point of the Coulomb explosion. Bandrauk *et al.* proposed a charge resonance enhanced ionization (CREI) model[11] and showed that there exists a pair of charge-resonant states that are strongly coupled to the laser field at a critical distance, R_c, where photoionization can be greatly enhanced. Based on this model, the energy defect ratio of all of the charged-state molecular ions is nearly the same. Researchers found that for a given molecule, the R_c is nearly the same for all charge states and is appropriately 1–2 times larger than the equilibrium internuclear distance of the neutral molecule.[9,12]

Until now, the CREI model has been proved to be an appropriate explanation for highly charged molecular ions. However, George N. Gibson *et al.*[13,14] proposed that CREI experience a sequential ionization process where electrons are successively stripped in one laser pulse and the nuclear stretch cannot be avoided. The kinetic energy (KE) obtained from each channel also included the energy accumulated from the previous ionization step. Therefore, the R_c should change along with the charge states rather than having a fixed value for all of the charge states for a given molecule. In addition, the ionization process is greatly influenced by the intensity and the duration of the laser pulse.

The existence of the R_c can resolve the energy deficit problem for the Coulomb explosion (CE) process. However, the driving force of these dissociation processes and how the KE accumulated in the molecules before dissociation is still worth researching. In this work, we studied the dissociative ionization and CE of a Cl_2 molecule irradiated by an 800 nm femtosecond laser field using a de-sliced ion imaging technique. By measuring the KE of the fragment ions, we found that the molecular ions, Cl_2^+, dissociated from two excited states, $^2\Pi_u$ and $^2\Sigma_g^+$, with the electrons being respectively excited from the HOMO−1 and HOMO−2 orbital. For multi-charged molecular ions, Cl_2^{n+} (n = 2–8), an energy defect also existed in our

[a]*Key Laboratory of Science and Technology of Eco-Textiles, Ministry of Education, College of Chemistry, Chemical Engineering and Biotechnology, Donghua University, Shanghai 201620, China*

[b]*Department of Physics, State Key Laboratory of Precision Spectroscopy, East China Normal University, Shanghai 200062, People's Republic of China. E-mail: yyang@lps.ecnu.edu.cn*

experimental results, which could be explained by the CREI model. The measured KER of each channel for the Cl_2 Coulomb explosion was around 48–66% of the theoretical calculation. Our results showed that the stretch of the internuclear distance benefitted the ionization of the electrons to produce highly-charged molecular ions. In addition, other than the traditional CREI process, the critical distance, R_c, for the Cl_2 molecule in femtosecond laser fields was not a single point, but a short range that depended on the charge state.

Experimental and theoretical methods

The photodissociative ionization of the Cl_2 molecule in a near-infrared femtosecond laser field was performed in a home-made DC-sliced-velocity-imaging system, which has been described in detail elsewhere.[15] Briefly, the linearly polarized femtosecond laser pulse (70 fs FWHM, center wavelength: 800 nm) was focused into a custom DC-sliced imaging spectrometer by a biconvex lens with 40 cm focal length. The gaseous chlorine molecules that were seeded into helium (1 : 10) were ejected into the reaction chamber ($\sim 4.0 \times 10^{-9}$ mbar) by a pulse valve (General valve, Parker) with a repetition rate of 100 Hz and a duration of 150 μs. The laser beam interacted with a supersonic molecular beam at a right angle. The produced ions passing through the velocity mapping lens, during which momentum focusing was maintained and every individual ion-cloud was stretched to meet the slice condition, were detected by a pair microchannel plates (MCP) coupled with a P47 phosphor screen. The 2D momentum images of each fragment were the central slice (around $p_z = 0$) of the corresponding 3D momentum distribution and were obtained by a charge coupled device camera (PI-MAXII, Princeton Instrument) with a 5 ns time resolution. The laser intensity in the focal volume was estimated to be between 7×10^{13} to 1.0×10^{15} W cm^{-2}, which was calibrated by the relationship of the Ar^{2+}/Ar^{+} yield ratio and the laser intensity proposed by Guo *et al.*[16]

To better illustrate the ionization and dissociation process of the Cl_2 molecule, theoretical calculations were performed using the Gaussian 09 software package.[17] The potential energy surface (PES) was calculated with an equation-of-motion couple cluster singles and doubles (EOM-CCSD)[18–20] level of theory using an aug-cc-pvtz basis set.[21] The equation-of-motion couple cluster method has been identified to be an accurate method to calculate the energy of the excited states and has generally been used in singles and doubles excitation approximations. To verify the accuracy of this method, we compared the equilibrium distance of the ground state, $^2\Pi_g$, and excited states, $^2\Pi_u$ and $^2\Sigma_g^+$, of the Cl_2^+ ions as well as the energy gaps between them. The calculated equilibrium distance of the $^2\Pi_g$ and $^2\Pi_u$ states were 1.9 and 2.3 Å, respectively, which were in accordance with the reported data in ref. 22 (1.9 and 2.3 Å). The calculated energy gaps of these states were around 2.78 and 1.63 eV, which were very close to the same data (2.75 and 1.79 eV).[22] Therefore, the good agreement between our computation and previous results demonstrated the feasibility of the theoretical methodology used in this paper.

Results

The raw DC-sliced ion images of Cl^{n+} (n = 1–4) are shown in Fig. 1(a)–(d). Clearly, the multi-ring structure provided intuitive evidence that the fragment ions with the same charge state were from different reaction channels. The corresponding KE values were extracted and are shown in Fig. 1(e)–(h). The circles (**o**) denote the experiment data. The short dashed lines (**---**) are the fitting peaks and the solid line (—) is the simulated distribution. The label/channel (p, q) corresponds to the estimated dissociation process, $Cl_2^{(p+q)+} \rightarrow Cl^{p+} + Cl^{q+}$.

Based on the two-body CE model, the exploded two fragment ions should have met the momentum conservation requirements. Therefore, the relationship of the KERs and mass can be written as

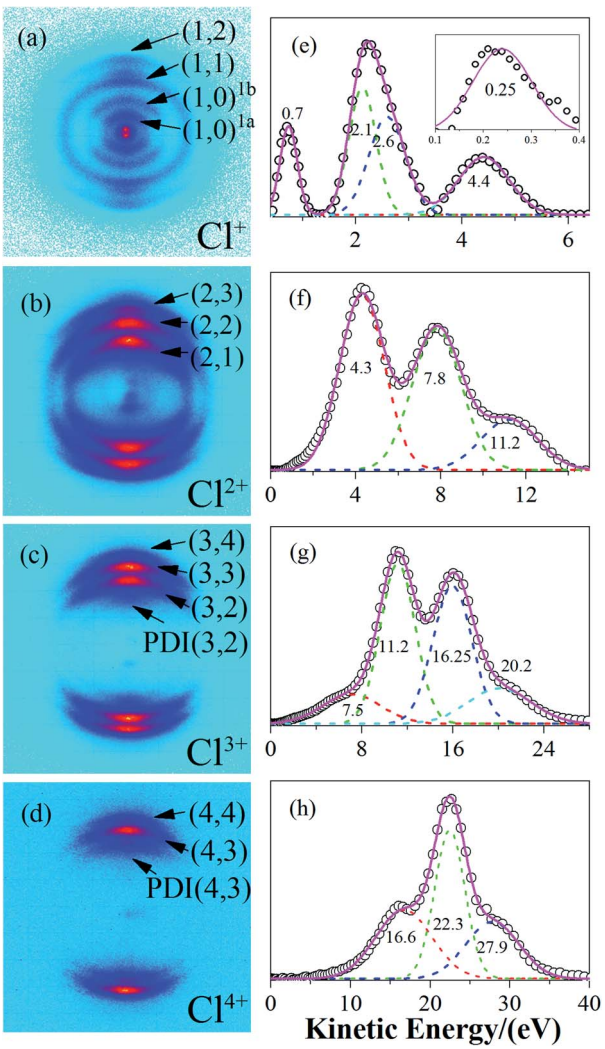

Fig. 1 The sliced images of the fragment ions, Cl^+, Cl^{2+}, Cl^{3+} and Cl^{4+} as well as their kinetic energy release distribution. The circle (**o**) denotes the experiment data, the short dashed lines (**---**) are the fitting peaks, and the solid line (—) is the simulated distribution. The channel (p, q) corresponds to the estimated dissociation process $Cl_2^{(p+q)+} \rightarrow Cl^{p+} + Cl^{q+}$.

$$\frac{E_{kin}(Cl^{p+})}{E_{kin}(Cl^{q+})} = \frac{m(Cl^{q+})}{m(Cl^{p+})} \quad (1)$$

where, E_{kin} is the KE of the fragment ion, m is the mass, and p and q represent the charge states of the two fragment ions. Considering the limit of the experimental condition and the data processing, the error factor, <5%, indicated that the two fragments were from the same CE channel. According to eqn (1), the estimated CE channels for the molecular ions, Cl_2^{n+} (n = 2–8), with the measured kinetic energy releases (KERs) are listed in Table 1. The dissociative ionization channels (1, 0)[1a] and (1, 0)[1b] from Cl_2^+ are also listed in Table 1.

Discussion

(1) Dissociative ionization of the (1, 0) channel

At a relatively lower laser intensity, the single ionization dominated the ionization process of the Cl_2 molecule and the subsequent dissociation produced one Cl^+ ion and one neutral Cl atom. Two dissociation channels with different KERs for the Cl_2^+ dissociation were observed and marked as channel (1, 0)[1a] and channel (1, 0)[1b]. As shown in Table 1, because the KERs of the above two channels were much smaller than those from the CE channels, these Cl^+ ions could not be produced by the CE process of the multi-charged molecular ions. In addition, the energy difference of these two channels was 0.9 eV, which was far beyond our experimental systematic error. Therefore, the two channels should have given rise to the dissociation process of the Cl_2^+ ions with different excited electronic states. To further understand the dissociation process, the PES of the Cl_2^+ ion was calculated and is shown in Fig. 2.

Fig. 2 shows the PES of the Cl_2^+ ions by removing one electron from the HOMO, HOMO−1 and HOMO−2 orbital of the Cl_2 molecule, respectively. After removing one electron from the HOMO, the molecule was excited to the $^2\Pi_g$ state. Considering HOMO is an anti-bonding π orbital, the equilibrium internuclear distance of the Cl_2^+ ion (1.90 Å) was shorter than that of the Cl_2 molecule (1.98 Å). The interaction of the two Cl atoms became stronger as shown in Fig. 2b and the potential well became deeper. The situation was the opposite when the removed electron was from the HOMO−1 and the molecular ion

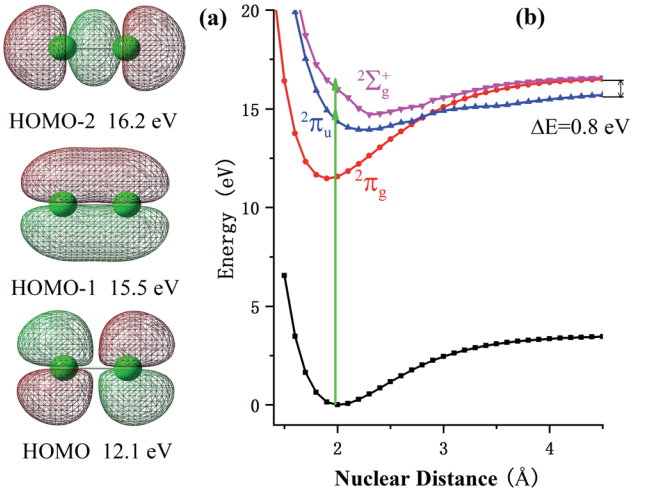

Fig. 2 (a) Molecular orbitals and the corresponding vertical ionization energy of Cl_2 calculated at the EOM-CCSD level of theory using the aug-cc-pvtz basis set with the Gaussian 09 software. The green balls represent the Cl atoms. (b) Calculated PES of the Cl_2 molecule as well as the ground state and several excited states of the Cl_2^+ ions. For the Cl_2^+ ions, the $^2\Pi_g$, $^2\Pi_u$ and $^2\Sigma_g^+$ states were formed by respectively removing one electron from the HOMO, HOMO−1 and HOMO−2 orbital.

Table 1 Dissociation channels for the Cl_2^{n+} molecular ions (n = 1–8) with the measured KERs (eV)

	Dissociation channels	KERs
(1, 0)[1a]	$Cl_2^+ \rightarrow Cl^+ + Cl$	0.5
(1, 0)[1b]	$Cl_2^+ \rightarrow Cl^+ + Cl$	1.4
(1, 1)	$Cl_2^{2+} \rightarrow Cl^+ + Cl^+$	4.8
(2, 1)	$Cl_2^{3+} \rightarrow Cl^{2+} + Cl^+$	8.7
(2, 2)	$Cl_2^{4+} \rightarrow Cl^{2+} + Cl^{2+}$	15.6
(3, 2)	$Cl_2^{5+} \rightarrow Cl^{3+} + Cl^{2+}$	22.4
PDI(3, 2)	$Cl_2^{5+} \rightarrow Cl^{3+} + Cl^{2+}$	15.0
(3, 3)	$Cl_2^{6+} \rightarrow Cl^{3+} + Cl^{3+}$	32.5
(4, 3)	$Cl_2^{7+} \rightarrow Cl^{4+} + Cl^{3+}$	42.5
PDI(4, 3)	$Cl_2^{7+} \rightarrow Cl^{4+} + Cl^{3+}$	33.8
(4, 4)	$Cl_2^{8+} \rightarrow Cl^{4+} + Cl^{4+}$	55.8

was excited to the $^2\Pi_u$ state. The HOMO−1 was a bonding orbital. Removing one electron from the bonding orbital made the equilibrium internuclear distance longer to 2.3 Å. The interaction of the two Cl atoms weakened and the potential well became shallower. The removed electron could have also come from the σ_g orbital (HOMO−2) to form the $^2\Sigma_g^+$ state. The PES of this state was similar to the $^2\Pi_u$ state with a long equilibrium internuclear distance and weak interactions.

The dissociative ionization started from the neutral Cl_2 molecule being vertically ionized at the equilibrium internuclear distance (green region in Fig. 2b) to produce the Cl_2^+ ion. The $^2\Pi_g$ state was right in its potential well, where the molecular ions were barely able to dissociate into fragments. Our experimental results, in which no fragments dissociated from the $^2\Pi_g$ state, also support this point.

Actually, the Cl_2^+ ions were easy to populate in the Cl_2^+ ion state $^2\Pi_g$ due to the low exciting energy and bounding character. The molecular ion on this state may not have dissociated directly, but these ions may have been further excited to a higher state and produced multi-charge fragment ions, which we discussed in previous reports.[23]

When the Cl_2^+ ions are vertically excited to $^2\Pi_u$ and $^2\Sigma_g^+$ states, during which the electrons are respectively taken away from the HOMO−1 and HOMO−2 orbital, the molecular ions populate on high vibrationally excited states that have enough energy to overcome the potential well. Therefore, they have the chance to dissociate into fragments. There were only two channels observed for Cl_2^+ dissociation and the measured energy difference of these two channels was 0.9 eV (0.5 eV and 1.4 eV). Therefore, they dissociated from the two states with an energy gap around 0.9 eV. By observing the PES of the two states, we found that the energy gap of the $^2\Pi_u$ and $^2\Sigma_g^+$ states

was 0.8 eV, which was similar to our experimental results. Considering the experimental systematic error, we concluded that channel 1a and channel 1b dissociated from the $^2\Pi_u$ and $^2\Sigma_g^+$ states of the Cl_2^+ ions, respectively.

(2) CE of multi-charged molecular ions Cl_2^{n+} (n = 2–8)

When the Cl_2 molecule was irritated by an intense femtosecond laser field, several electrons may be peeled off to produce the multi-charged molecular ions Cl_2^{n+} (n = 2–8). The repulsion of the multiple charges drove the dissociation process for the Cl_2^{n+} (n = 2–8) ions. For the diatomic molecule CE channels $Cl_2^{(p+q)+} \rightarrow Cl^{p+} + Cl^{q+}$, the possible dissociation pathways of the multi-charged parent ions included a charge symmetry dissociation (CSD) where $|p - q| \leq 1$, and a charge asymmetric dissociation (CAD) where $|p - q| > 1$. According to our experimental results, the latter case was not observed and it is likely that the CAD process was not involved in our experiment.

In classic CE model, the total KERs of one CE channel are expressed as:

$$\mathrm{KER} = 14.4\ pq/r \tag{2}$$

where p and q represent the charge states of the fragment ions, and r indicates the internuclear distance in Å. Ideally, if the KERs can be measured accurately, then the critical distance, R_c, can be determined. In the CE model, the CE process is dominated by coulomb repulsion exclusively and neglects any other interaction in the molecular ions. For the molecular ions, Cl_2^{n+} (n = 3–8), the repulsion of the extra positive charges greatly exceeded the chemical bonding interaction and the chemical binding interaction could be neglected. Therefore, the PES exhibited a repulsive character, even in the short nuclear distance. Thus, we used the charge repulsive curve to analyze the CE process for molecular ions Cl_2^{n+} (n = 3–8). However, the chemical binding interaction played an important role in the dissociation process for low charge parent ions, Cl_2^{2+}, and influenced the R_c of the CE process. Therefore, the real PES of Cl_2^{2+} rather than the charge repulsive curve should be used to obtain the accurate critical distances. According to ref. 23, the PES of the ground state in a short nuclear distance exhibited a bounding character due to the chemical bonding interaction between the two chlorine atoms. Once the nuclear distance was over 3 Å, the chemical bonding interaction could be neglected and the repulsion between the two extra positive charges dominated the interaction process. Thus, the PES in the long nuclear distance exhibited a repulsive character.

Using the PES of the parent ions Cl_2^{n+} (n = 2–8), the critical distance, $R_{m,n}$, was calculated as follows. The relationship of the experimentally measured KERs, $E_{m,n}$, and the potential energy for the (m, n) channel, $V_{m,n}(R_{m,n})$, was used. They should meet the following relationship:[14,15]

$$E_{m,n}^{\mathrm{exp}} = V_{m,n}(R_{m,n}) - V(\infty) \tag{3}$$

where, V represents the potential energy, which we adjusted to make $V(\infty) = 0$. Then, the experimental KE equals the potential energy change before and after the CE process. However, the KERs that were accumulated from the previous steps were not included in eqn (3). Therefore, the accumulated KERs, $E_{m,n}^{\mathrm{acc}}$, should be added:

$$E_{m,n}^{\mathrm{exp}} = V_{m,n}(R_{m,n}) + E_{m,n}^{\mathrm{acc}} \tag{4}$$

For any ionization from (i, j) to (m, n), the KERs increment can be expressed as:

$$E_{m,n}^{\mathrm{exp}} - E_{i,j}^{\mathrm{exp}} = V_{m,n}(R_{m,n}) + E_{m,n}^{\mathrm{acc}} - V_{i,j}(R_{i,j}) - E_{i,j}^{\mathrm{acc}} \tag{5}$$

The accumulated energy increase from (i, j) to (m, n) can be seen in Fig. 3(the green line).

$$\Delta E = E_{m,n}^{\mathrm{acc}} - E_{i,j}^{\mathrm{acc}} = V_{i,j}(R_{i,j}) - V_{i,j}(R_{m,n}) \tag{6}$$

Substituting eqn (6) into eqn (5), we arrived at:

$$E_{m,n}^{\mathrm{exp}} - E_{i,j}^{\mathrm{exp}} = V_{m,n}(R_{m,n}) - V_{i,j}(R_{m,n}) \tag{7}$$

$V_{m,n}(R_{m,n})$ can be calculated according to Coulomb's law. Thus, eqn (7) can be written as:

$$E_{m,n}^{\mathrm{exp}} - E_{i,j}^{\mathrm{exp}} = k\frac{mn}{R_{m,n}} - k\frac{ij}{R_{m,n}} = k\frac{(mn - ij)}{R_{m,n}} \tag{8}$$

where k is 14.4 eV Å^{-1} and R is in Å.

We applied eqn (7) to our measured KERs data and the calculated R_c for each channel is listed in Table 2. For comparison, the traditional method (eqn (2)) was used to calculate the critical distance and the results are also listed as R_c^* in the table. We found that the values of R_c^* were always smaller than those of R_c.

Considering the molecular Cl_2 experience, a sequential ionization process where the electrons are successively stripped, all of the dissociation channels were charge symmetric. The only possible ionization step was (1, 1) → (1, 2) → (2, 2) → (2, 3) → (3, 3) → (3, 4) → (4, 4). The (1, 1) channel was produced by the Cl_2^+ ion, which further ionized to Cl_2^{2+}. According to our

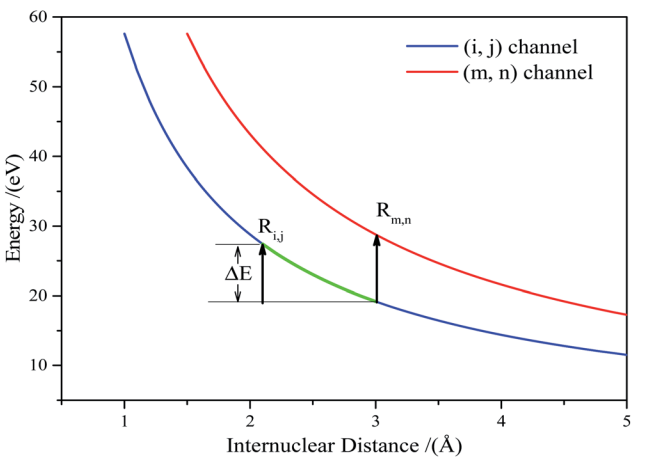

Fig. 3 The accumulated energy increase, ΔE, from the (i, j) channel to the (m, n) channel.

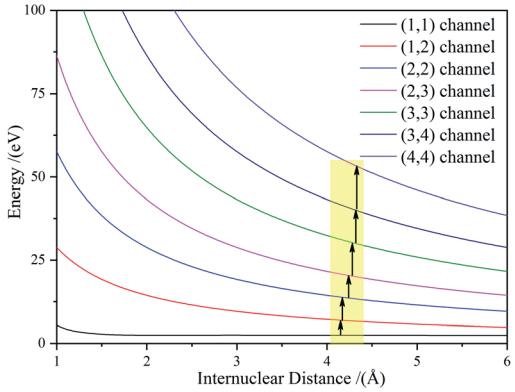

Fig. 4 Step-by-step ionization path.

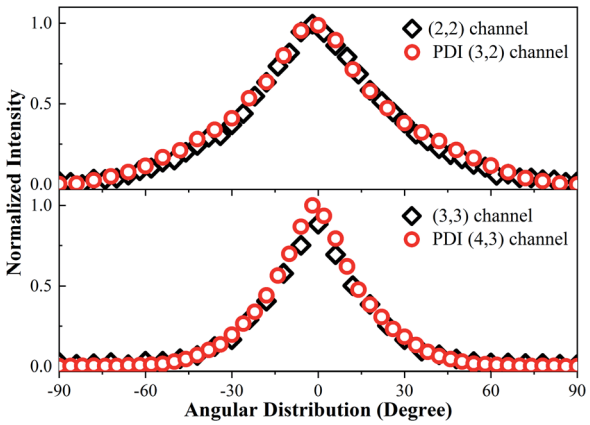

Fig. 5 The angular distribution of the (2, 2) channel, PDI (3, 2) channel, (3, 3) channel, and PDI (4, 3) channel.

Table 2 The calculated R_c based on a classic two-body model and the travel time, T_{tra}, for each channel

Channels	R_c (Å)	T (fs)	R_c^* (Å)
(1, 1) → (1, 2)	4.15	19.8	3.31
(1, 2) → (2, 2)	4.17	2.0	3.69
(2, 2) → (2, 3)	4.24	3.3	3.86
(2, 3) → (3, 3)	4.28	1.9	3.99
(3, 3) → (3, 4)	4.32	1.6	4.07
(3, 4) → (4, 4)	4.33	0.5	4.13

experimental results and the theoretical calculation, the CE of Cl_2^{2+} started at $R_c = 3$ Å and produced Cl^+ fragment ions with the KERs of the channel mainly distributed around 4.8 eV. During the nuclear distance stretch, Cl_2^{2+} was ionized to Cl_2^{3+} at $R_c = 4.15$ Å. Then, some of the Cl_2^{3+} ions exploded to produce Cl^{2+} and Cl^+ ions with a 8.7 eV KER. The measured KER included the potential energy change and the accumulated energy from the Cl_2^{2+} stretching process. The other Cl_2^{3+} ions reduplicated the above process at 4.17 Å for further ionization to Cl_2^{4+} ions. If the laser pulse intensity was high enough, Cl_2^{n+} (n = 3–8) ions were successfully produced, resulting in the generation of the CE channels listed in Table 2 and Fig. 4. We found that all of the high charged molecular ions were produced at R_c around 4.2 Å, which was consistent with the enhanced ionization mechanism. The difference was that the R_c was not a single point, but a small range.

Once these ionization and dissociation processes were determined, it was important to know whether the pulse duration was long enough to cover these multi-electron ionization process. We calculated the time it took (T_{ij-mn}) to travel from $R_{i,j}$ to $R_{m,n}$ on the $V_{i,j}(r)$ potential energy curve using eqn (9):

$$T_{ij-mn} = \int_{R_{i,j}}^{R_{m,n}} \frac{\mathrm{d}r}{\sqrt{\frac{4}{m}\left[V_{i,j}(R_{i,j}) - V_{i,j}(r)\right]}} \quad (9)$$

where r is the internuclear separation. The calculation results are listed in Table 2.

The travel time from the (1, 1) to (1, 2) channel was 19.8 fs, which was much longer than the further ionization process. The whole process from (1, 1) to (4, 4) was less than 30 fs. Considering that the (0, 1) to (1, 1) channel also took some time, the whole CE process was finished in one laser pulse duration of 70 fs.

(3) Post dissociation ionization

In Fig. 1c, we observed one component with the KER at 7.5 eV (the first peak in Fig. 1c), which we could not find a corresponding component to match. Considering that the whole CE process could be finished in one laser pulse and the experimental systemic error could not be so large, this low KE component may have been from the post-dissociation ionization[9] of the (2, 2) channel, which exploded to a Cl^{2+} ion first. The laser field was still present after the dissociation. Then, some Cl^{2+} ions with a 7.8 eV KE were further ionized to Cl^{3+} ions before they left the interaction zone. To verify our assumption, we compared the KE and angular distribution of this component and the Cl^{2+} ion in the (2, 2) channel. The 7.5 eV KE was very close to the 7.8 eV KE component in the (2, 2) channel. The 0.3 eV error may have been caused by the data collection process or an experimental systemic error. In addition, as shown in Fig. 5, the angular distribution of the two components is exactly the same, proving that the low KE Cl^{3+} ion was ionized from the Cl^{2+} ion. This same situation also took place in the Cl^{4+} ion, where the low 16.9 eV KE component was from the ionization of an exploded Cl^{3+} ion. This phenomenon indicated that the CE process was very fast and could take place in one laser pulse, which was 70 fs under our experimental conditions.

Conclusions

We studied the dissociative ionization and CE of a Cl_2 molecule in a near-infrared femtosecond laser field using a dc-sliced ion velocity imaging technique. We found that Cl_2^+ dissociates from two excited states, $^2\Pi_u$ and $^2\Sigma_g^+$, with electrons respectively from the HOMO−1 and HOMO−2 orbital. For the Cl_2^{n+} (n = 2–8) molecular ions, their precursor started to expend at the

equilibrium internuclear distance, R_e, and ionized at the critical distance, R_c, to explode into ionic fragments. The accumulated KERs were also included to calculate the final KERs. The R_c for these molecular ions was not a single point, but a small region around 4.2 Å. The dissociation time was calculated, which was within one pulse duration. This was further proved by observing the post dissociation ionization channels.

Conflicts of interest

The authors declare no competing financial interests.

Acknowledgements

This work was supported by the Natural Science Foundation of Shanghai (No. 16ZR1448100), the "Chenguang Program" by the Shanghai Education Development Foundation and Shanghai Municipal Education Commission (No. 16CG38), and the National Natural Science Foundation of China (No. 11604046).

References

1 Z. Wu, C. Wu, X. Liu, Y. Deng and Q. Gong, *J. Phys. Chem. A*, 2010, **114**, 6751.
2 V. Tagliamonti, H. Chen and G. N. Gibson, *Phys. Rev. A*, 2011, **84**, 043424.
3 H. Sakai, H. Stapelfeldt, E. Constant, M. Y. Ivanov, D. R. Matusek, J. S. Wright and P. B. Corkum, *Phys. Rev. Lett.*, 1998, **81**, 2217.
4 R. J. Verver, D. R. Matusek, J. S. Wright, G. N. Gibson, R. Bhardwaj, S. Aseyev, D. M. Villeneuve, P. B. Corkum and M. Y. Ivanov, *J. Phys. Chem. A*, 2001, **105**, 2435.
5 T. Seideman, M. Y. Ivanov and P. B. Corkum, *Phys. Rev. Lett.*, 1995, **75**, 2819.
6 F. Rosca-Pruna, E. Springate, H. L. Offerhaus, M. Krishnamurthy, N. Farid, C. Nicole and M. J. J. Vrakking, *J. Phys. B: At., Mol. Opt. Phys.*, 2001, **34**, 4919.
7 P. A. Hatherly, M. Stankiewiczt, K. Codling, L. J. Frasinski and G. M. Cross, *J. Phys. B: At., Mol. Opt. Phys.*, 1994, **27**, 2993.
8 J. McKenna, *et al.*, *Phys. Rev. A*, 2006, **73**, 043401.
9 M. Schmidt, D. Normand and C. Cornaggia, *Phys. Rev. A*, 1994, **50**, 5037.
10 S. Chelkowski and A. D. Bandrauk, *J. Phys. B: At., Mol. Opt. Phys.*, 1995, **28**, L723.
11 T. Zuo and A. D. Bandrauk, *Phys. Rev. A*, 1995, **52**, R2511.
12 J. H. Posthumusy, A. J. Gilesy, M. R. Thompsony, W. Shaikhz, A. J. Langleyz, L. J. Frasinskiy and K. Codling, *J. Phys. B: At., Mol. Opt. Phys.*, 1996, **29**, L525.
13 J. P. Nibarger, S. V. Menon and G. N. Gibson, *Phys. Rev. A*, 2001, **63**, 053406.
14 S. V. Menon, J. P. Nibarger and G. N. Gibson, *J. Phys. B: At., Mol. Opt. Phys.*, 2002, **35**, 2961.
15 Y. Yang, *et al.*, *J. Chem. Phys.*, 2011, **135**, 064303.
16 C. Guo, M. Li, J. P. Nibarger and G. N. Gibson, *Phys. Rev. A*, 1998, **58**, R4271.
17 M. J. Frisch*et al.*, *Gaussian 09*, Gaussian, Inc., Wallingford CT, 2009.
18 J. F. Stanton and R. J. Bartlett, *J. Chem. Phys.*, 1993, **98**, 7029.
19 M. Caricato, *J. Chem. Phys.*, 2013, **139**, 114103.
20 M. Kállay and J. Gauss, *J. Chem. Phys.*, 2004, **121**, 9257.
21 D. E. Woon and T. H. Dunning, *J. Chem. Phys.*, 1992, **98**, 1358.
22 S. D. Peyerimhoff and R. J. Buenker, *Chem. Phys.*, 1981, **57**, 279.
23 J. Zhang, Y. Yang, Z. Li, H. Sun, S. Zhang and Z. Sun, *Phys. Rev. A*, 2018, **98**, 043402.